

General Disclaimer

One or more of the Following Statements may affect this Document

- This document has been reproduced from the best copy furnished by the organizational source. It is being released in the interest of making available as much information as possible.
- This document may contain data, which exceeds the sheet parameters. It was furnished in this condition by the organizational source and is the best copy available.
- This document may contain tone-on-tone or color graphs, charts and/or pictures, which have been reproduced in black and white.
- This document is paginated as submitted by the original source.
- Portions of this document are not fully legible due to the historical nature of some of the material. However, it is the best reproduction available from the original submission.

NASA Technical Memorandum 79071

(NASA-TM-79071) APPLICATIONS OF VELOCITY
POTENTIAL FUNCTION TO ACOUSTIC DUCT
PROPAGATION AND RADIATION FROM INLETS USING
FINITE ELEMENT THEORY (NASA) 12 p HC A02/MF
A01

N79-15959

Unclass

CSCS 21E G3/07 13789

APPLICATIONS OF VELOCITY POTENTIAL
FUNCTION TO ACOUSTIC DUCT PROPAGATION
AND RADIATION FROM INLETS USING FINITE
ELEMENT THEORY

K. J. Baumeister
Lewis Research Center
Cleveland, Ohio

and

R. K. Majjigi
General Electric Co.
Cincinnati, Ohio



TECHNICAL PAPER to be presented at the
Fifth Aeroacoustics Conference
sponsored by the American Institute of Aeronautics and Astronautics
Seattle, Washington, March 12-14, 1979

APPLICATIONS OF VELOCITY POTENTIAL FUNCTION TO ACOUSTIC DUCT PROPAGATION AND RADIATION FROM INLETS USING FINITE ELEMENT THEORY

K. J. Baumeister
NASA-LERC, Cleveland, Ohio
and
R. K. Majjigi
GE Cincinnati, Ohio

Abstract

A finite element velocity potential program has been developed for NASA Lewis at the Georgia Institute of Technology to study acoustic wave propagation in complex geometries. For irrotational flows, relatively low sound frequencies, and plane wave input, the finite element solutions show significant effects of inlet curvature and flow gradients on the attenuation of a given acoustic liner in a realistic variable area turbofan inlet. In addition, as shown in the paper, the velocity potential approach can not be used to estimate the effects of rotational flow on acoustic propagation since the potential acoustic disturbances propagate at the speed of the media in sheared flow. Approaches are discussed that are being considered for extending the finite element solution to include the far field as well as the internal portion of the duct. A new matrix partitioning approach is presented that can be incorporated in previously developed programs to allow the finite element calculation to be marched into the far field. The partitioning approach provides a large reduction in computer storage and running times.

Introduction

When using numerical techniques in calculating acoustic waves propagating in ducts (such as finite elements in Refs. 1 to 3 and finite differences in Refs. 4 to 6) the velocity potential formulation of the acoustic wave equation¹ offers many advantages over the conventional linearized gas equation.² For two dimensional flows, the velocity potential approach reduces the computer storage and running time by an order of magnitude compared to the more general linearized gas equation approach. Since the flow into an inlet is usually modeled by potential flow (excluding the boundary layer), the acoustic velocity potential is ideally suited for acoustic inlet calculations.

On the other hand, when rotational flow exists in the inlet (wall and centerbody boundary layers), the accuracy of a potential flow calculation is questionable. The first purpose of this paper was to investigate the limitations of shear on the potential flow formulation and to suggest a means of extending the potential flow finite element analysis to incorporate sheared flow. A second purpose of this paper was to determine the sensitivity of an acoustic liner to variations in area and flow experienced in a typical engine inlet.⁷ This was accomplished using the finite element velocity potential computer program developed by the Georgia Institute of Technology for NASA Lewis Research Center written under NASA Lewis grant (NAS-3036).

Finally, finite elements can simultaneously include both the far field and internal ducting of a turbofan engine. For example, in the absence of flow, a formulation of a finite element approach

for sound propagation in the near field of an infinite baffle with an embedded circular piston was presented in Ref. 8. Although the finite element approach is relatively easy to formulate, core storage requirements and long run times presently prevent the application of the finite element approach to simultaneously including both the inlet and far field in a single calculation. In Ref. 1, for example, by structuring the column matrix of modal unknowns to successively be the real and then the imaginary part of the acoustic potential at a node, the global matrix is well banded. Even so, the formulation of Ref. 1 was limited to 270 elements. Reference 3 improved the matrix structure by using a complex solution technique which reduced the bandwidth of the matrix even further; however, 150 total elements were the maximum quoted in the paper.

The third purpose of this paper, therefore, is to discuss current work for extending finite element velocity potentials from the internal portion of the duct into the far field. In particular, a new numerical partitioning method is presented which is suited for extending the solution from the internal portion of the duct into the far field.

Nomenclature

C_1	constant of integration, N/m^2 (Eq. (22))
C_2, C_3	constants of integration, m/sec (Eqs. 23 and 24)
c_0	velocity of sound, m/sec
D_0	diameter at rotor position, m
f	frequency, Hz
H	height of duct, m
i	$\sqrt{-1}$
K	number of grid points in axial direction
L	length of duct, m
M	Mach number of axial mean flow, U/c_0
m	spinning mode number
p	acoustic pressure, $p(x,y,t)$, N/m^2
P_0	entrance acoustic pressure, $p_0(x,y,t)$, N/m^2
p^0	spatial acoustic pressure, $p^0(x,y)$, N/m^2
r	radial coordinate, m
t	time, sec
U	axial mean flow velocity, $U(x,y)$, m/sec
u	acoustic axial velocity, $u(x,y,t)$, m/sec
u^0	spatial acoustic axial velocity, $u^0(x,y)$, m/sec
V	transverse mean flow velocity, $V(x,y)$, m/sec
v	acoustic transverse velocity, $v(x,y,t)$, m/sec
v^0	spatial acoustic transverse velocity, $v^0(x,y)$, m/sec
x	axial coordinate, m
y	transverse coordinate, m
Z	impedance, $g/cm^2 sec$
Z_{eff}	effective impedance, $g/cm^2 sec$
z	axial position
ζ	specific acoustic impedance

η	dimensionless frequency $D_0 f/c_0$ or Hf/c_0
θ	angular position, radians
ρ_0	density, g/m^3
Φ	steady potential function, $\Phi(x,y)$, m^2/sec
Φ^*	potential function, $\Phi^*(x,y,t)$, m^2/sec
φ	acoustic potential function, $\varphi(x,y,t)$, m^2/sec
φ^0	spatial acoustic potential function, $\varphi^0(x,y)$, m^2/sec
ω	angular frequency, rad/sec

Subscripts:

()_x derivatives with respect to x (similar for y and t)

Sheared Mean Flow

Rotational velocity fields exist for sheared viscous flows in the inlet along the walls of a turbofan cowl and along its centerbody. The complete acoustic equations for sheared viscous flows were developed by Mungar and Gladwell.⁹ By common practice, the viscous terms in the linearized acoustic equations are neglected and the inviscid acoustic equations are solved using the mean flow velocities that result from a consideration of viscosity only on the mean flow field. Similarly, because of the significant computational advantage of the acoustic potential formulation, it would be desirable if the existing potential wave program could be extended to include boundary layer flows. First, the fully irrotational acoustic flow equations will be presented. Next, this paper will develop the acoustic flow equations for a rotational mean flow field with an irrotational acoustic field. The consequence of such an assumption is discussed and conclusions are made about the use of the acoustic potential function to model sheared flows.

Irrotational Mean and irrotational Acoustic Flow Fields

For two dimensional flows, the velocity potential representation of the inviscid momentum and mass continuity equations can be written as (Ref. 10, pg. 76).

$$\Phi_{tt}^* + 2\Phi_x^* \Phi_{xt}^* + 2\Phi_y^* \Phi_{yt}^* + \Phi_x^{*2} \Phi_{xx}^* + 2\Phi_x^* \Phi_y^* \Phi_{xy}^* + \Phi_y^{*2} \Phi_{yy}^* = c_0^2 \Phi_{xx}^* + c_0^2 \Phi_{yy}^* \quad (1)$$

where Φ^* is the velocity potential. The symbols are defined in the list of symbols. To keep the analysis simple, the rectangular coordinate system is used rather than a more general coordinate system. The velocity potential Φ^* is assumed to be composed of a steady potential Φ and an acoustic potential φ :

$$\Phi^*(x,y,t) = \Phi(x,y) + \varphi(x,y,t) \quad (2)$$

The mean flow velocities are of the form

$$U = \Phi_x = U(x,y) \quad (3)$$

$$V = \Phi_y = V(x,y) \quad (4)$$

and a constant speed of sound c_0 is assumed. With these assumptions, and by dropping those terms which according to the assumption of small perturba-

tion, may be regarded as negligible compared to the remaining terms, Eq. (1) reduces to

$$\begin{aligned} (1 - M^2)\Phi_{xx} + \Phi_{yy} - 2 \frac{M}{c_0} \Phi_{xt} \\ - 2M \frac{\partial M}{\partial y} \Phi_y - \frac{1}{c_0^2} \Phi_{tt} \\ = \frac{V^2}{c_0^2} \Phi_{yy} + \frac{2V}{c_0^2} \Phi_{yt} + \frac{2V}{c_0} \frac{\partial M}{\partial y} \Phi_x \\ + 2M \frac{V}{c_0} \Phi_{xy} + 2 \frac{V}{c_0^2} \frac{\partial V}{\partial y} \Phi_y \end{aligned} \quad (5)$$

where the mean flow velocities are related by the irrotationality condition

$$c_0 \frac{\partial M}{\partial y} = \frac{\partial V}{\partial x} \quad (6)$$

Parallel shear flow with $M(y)$ and $V = 0$ is used to approximate boundary layer flows. In this case, Eq. (5) reduces to

$$\begin{aligned} (1 - M^2)\Phi_{xx} + \Phi_{yy} - 2 \frac{M}{c_0} \Phi_{xt} \\ - 2M \frac{\partial M}{\partial y} \Phi_y - \frac{1}{c_0^2} \Phi_{tt} = 0 \end{aligned} \quad (7)$$

However, Eq. (7) violates the irrotationality assumption which was used to establish Eq. (1) since Eq. (6) is no longer satisfied. Could, however, Eq. (7) be used to approximate a shear flow field? Equation (7) is similar to the Pridmore-Brown (Ref. 11) shear flow equation, except the Pridmore-Brown equation has two dependent variables. When the wave equation is expressed in one dependent variable, it becomes third order (Ref. 12, Eq. 1.22, pg. 9). Therefore Eq. (7) may alter the true physics of the acoustic propagation. It would be difficult to evaluate the effect of this approximation from numerical solutions. Consequently, a derivation will now be made assuming an acoustic potential in a parallel sheared mean flow so that Eq. (7) can be evaluated.

Rotational Mean Flow and Irrotational Acoustic Propagation

Because of the significant computational advantages of the acoustic potential formulation, an attempt will be made to extend the existing potential wave program to include the case of boundary layer flows that exist along the engine walls and centerbodies. To do this in a rigorous manner, one starts with the linearized gas dynamic equations for a rotational flow field.

For the simple case of a rectangular coordinate system and isentropic ($p = c_0^2 \rho$) parallel sheared mean flow ($U = U(y)$; $V = 0$), the governing gas dynamic equations¹³ become

Continuity

$$\frac{\partial \rho}{\partial t} + U \frac{\partial \rho}{\partial x} + \rho_0 c_0^2 \left(\frac{\partial u}{\partial x} + \frac{\partial v}{\partial y} \right) = 0 \quad (8)$$

x-momentum

$$\frac{\partial u}{\partial t} + u \frac{\partial u}{\partial x} + v \frac{\partial u}{\partial y} = -\frac{1}{\rho_0} \frac{\partial p}{\partial x} \quad (9)$$

y-momentum

$$\frac{\partial v}{\partial t} + u \frac{\partial v}{\partial x} = -\frac{1}{\rho_0} \frac{\partial p}{\partial y} \quad (10)$$

A solution to Eqs. (8) to (10) will, of course, require greater computer storage and operating time than Eq. (7) since the number of dependent variables has increased from one (ψ) to three (p, u, v). Now, the mean flow is considered to be rotational and the acoustic field is assumed to be irrotational such that

$$u = \frac{\partial \psi}{\partial x} \quad (11)$$

$$v = \frac{\partial \psi}{\partial y} \quad (12)$$

This assumption reduces Eqs. (8) to (10) to

$$\frac{\partial p}{\partial t} + u \frac{\partial p}{\partial x} + c_0^2 \rho_0 (\varphi_{xx} + \varphi_{yy}) = 0 \quad (13)$$

$$\varphi_{tx} + u \varphi_{xx} + \varphi_y \frac{\partial u}{\partial y} = -\frac{1}{\rho_0} \frac{\partial p}{\partial x} \quad (14)$$

$$\varphi_{ty} + u \varphi_{xy} = -\frac{1}{\rho_0} \frac{\partial p}{\partial y} \quad (15)$$

Equations (13) to (15) can not be combined to obtain a second order differential wave equation in the dependent variable. However, differentiating Eq. (14) with respect to y and Eq. (15) with respect to x and subtracting one equation from the other yields

$$(\varphi_{xx} + \varphi_{yy}) \frac{\partial u}{\partial y} + \varphi_y \frac{\partial^2 u}{\partial y^2} = 0 \quad (16)$$

which is the governing equation for describing an irrotational acoustic disturbance in a parallel mean shear flow. Since Eq. (16) contains no derivatives with respect to time, the irrotationality assumption changes the nature of the propagation equation.

The significance of Eq. (16) can be clearly understood by considering the simple case of a linear shear profile ($\partial^2 u / \partial y^2 = 0$). In this simpler but practical case, Eq. (16) reduces to

$$\varphi_{xx} + \varphi_{yy} = 0 \quad (17)$$

or if a harmonic time dependence is assumed

$$\varphi = \varphi^0 e^{-i\omega t} \quad (18)$$

then

$$\varphi_{xx}^0 + \varphi_{yy}^0 = 0 \quad (19)$$

Thus, the governing equation for the velocity potential becomes Laplace's equation, which indicates a diffusive propagation rather than a wave like propagation. The effect of this propagation on p and the acoustic velocities will now be considered.

The continuity equation, Eq. (13), simplifies by the use of Eq. (17) to

$$\frac{\partial p}{\partial t} + u \frac{\partial p}{\partial x} = 0 \quad (20)$$

Again, assuming that $p = p^0 e^{-i\omega t}$, Eq. (20) yields

$$p^0 + i \frac{u}{\omega} \frac{\partial p^0}{\partial x} = 0 \quad (21)$$

For a plane pressure wave at $x = 0$, a solution for p^0 from Eq. (21) is simply

$$p^0 = C_1 e^{i\omega x / U} \quad (22)$$

Similarly assuming $u = u^0 e^{-i\omega t}$ and $v = v^0 e^{-i\omega t}$ and substituting Eq. (22) into Eqs. (14) and (15) yields after integration

$$u^0 = e^{i\omega x / U} \left[C_3 - \frac{C_1 i \omega x}{\rho_0 U^2} - \frac{1}{U} \frac{\partial u}{\partial y} \left(C_2 x + \frac{i C_1 \omega x^2}{6 \rho_0 U^3} \frac{\partial u}{\partial y} \right) \right] \quad (23)$$

$$v^0 = e^{i\omega x / U} \left(C_2 + \frac{i C_1 \omega}{2 \rho_0 U^3} \frac{\partial u}{\partial y} x^2 \right) \quad (24)$$

These solutions of the continuity and momentum eq. ns have lead to the fact that

$$p, u, v, \propto e^{i\omega x / U} \quad (25)$$

that is, only forward propagating perturbation pressure p and velocities will exist and they will propagate at the speed of the medium flow U . Therefore, Eq. (16) does not have an acoustic solution, consequently, the potential flow solution cannot be used to estimate the effects of shear even in an approximate manner.

For the case of boundary layer flow, however a procedure based on the Goldstein-Rice analysis¹⁴ might be used for predicting the attenuation with shear flow in conjunction with the potential finite element method for turbofan inlets. For a linear shear layer, the impedance at the wall can be transformed into an effective impedance, Z_{eff} , at the edge of the boundary layer. This effective impedance could be used as the boundary condition for the potential flow calculation. The procedure is approximate because the calculation assumes a uniform boundary layer in the axial direction. For a growing boundary layer, the transform could be assumed to apply locally. In any event, this procedure represents a simple effective way of accounting for shear with a potential flow program.

Attenuation Sensitivity to Variable Area

The theory used for the design of acoustic liners for turbofan inlets without splitter rings has used a cylindrical duct for a model. As mentioned earlier, the present paper will estimate the sensitivity of duct attenuation to inlet curvature, centerbody and flow gradients (irrotational) for a typical turbofan inlet. To accomplish this task, a number of acoustic calculations are performed on the soft-walled turbofan inlet shown in Fig. 1.

This inlet geometry is similar to the QCSEE (quiet, clean, short-haul experimental engine) inlet which was designed to suppress inlet-emitted engine machinery noise using a high throat Mach number and thus has somewhat more curvature than a conventional inlet. In this case, the velocity potential finite element program of Ref. 1 was modified to include quadratic elements.

The governing equations in the program are developed from the axisymmetric cylindrical coordinate form of Eqs. (1) to (6). The exact form of φ is

$$\varphi(r, \theta, z, t) = \varphi^0(r, z) e^{-i(\omega t - m\theta)} \quad (26)$$

The detailed governing equations will not be presented here since they are fully documented in Ref. 1. Boundary layers are not considered in the calculation because, as was just shown, the program is limited to only irrotational flow fields.

At the present time, the frequency range and radial mode content is limited by the maximum number of elements which the computer can handle. The analysis considers plane wave input with dimensionless frequencies of η up to 2. In this case, seven elements were used to resolve the radial modes and fourteen elements were used to resolve axial variations. The acoustic design of an actual inlet will, of course, consider much higher frequencies. Unfortunately, at the present time finite element schemes can not handle high frequencies. Therefore, this analysis only investigates low frequency noise in variable area inlets. This might be corrected by adapting the wave envelope technique of Ref. 6 to this problem. The wave envelope technique can handle high frequencies with much fewer elements.

Attenuation calculations for a variable area inlet, a straight open cylinder and a bellmouth (Fig. 2) all with an L/D of 1 are presented in Fig. 3. The ratio of treatment length to duct diameter in these cases is 0.5. The soft wall extends over half the length of the duct beginning at the nose of the centerbody. With this geometry, the infinite uniform cylindrical duct model could be expected to give a reasonable estimate of the attenuation. The results displayed in Fig. 3 are for no mean flow. The effects of flow will be considered later. The impedance values chosen are the same for each inlet at a particular frequency. They are listed in Fig. 3. The impedance values chosen in the calculation approximate the optimum impedance (max. attenuation) for a plane pressure wave input into a long circular duct. A plane acoustic velocity is used as the source with a $\rho_0 c_0$ exit impedance.

The effect of inlet curvature and the centerbody on the duct attenuation can be ascertained by comparison of the various curves in Fig. 3 representing each inlet. The cylinder and bellmouth inlets give approximately the same attenuation as a function of frequency. Since the bellmouth is of uniform circular geometry, the effect of the short centerbody on the results appears to be insignificant in this no flow situation. The large area variation of the other inlet, however, does significantly affect the results. This suggests that reflections in this inlet may be important.

Figure 4 compares preliminary attenuation calculations for the variable area inlet and a cylin-

drical inlet in a flow situation. The fan plane Mach number for the variable area inlet was 0.52 with an average Mach number of 0.579 at the soft wall section of the inlet, as calculated by one-dimensional isentropic gas dynamic relations. The Mach number in the cylinder was also chosen to be 0.579. The impedance values used in these calculations were those listed in Fig. 3 divided by $(1 - M)^2$ with M equal to 0.579. Again, as seen in Fig. 4, the QCSEE inlet differs considerably from the cylinder results.

In Fig. 4, the flattening of the cylinder attenuation curve probably results because the impedance values chosen are not at the optimum for this Mach number. However, the important point is that for the same value of impedance, area variations can significantly change the calculated attenuation.

Far Field Radiation

As mentioned in the introduction, this section will be concerned with current ideas for extending finite elements from the internal portion of the duct into the far field. Under a three year extension of NASA Lewis grant NAS-3036, which will run from 11/78 to 10/81, Professors Zinn and Sigman will be developing methods for extending their finite element analysis into the far field. First, a small effort will be devoted to more accurately and efficiently specifying the steady flow field around an inlet in a form compatible with the acoustic calculations. However, the majority of the work effort in this grant will be devoted towards the calculation of acoustic properties of the inlet and the associated external region.

The direct extension of finite elements into the far field is illustrated in Fig. 5. The number of elements greatly increases the further the analysis is carried from the inlet. Therefore, this approach requires very efficient ways of storing and solving the finite element global matrix. Considerable effort should be devoted to the direct method, since improved handling of the elements will benefit far field approaches as well as improve capabilities for present induct analysis. As mentioned earlier, to handle higher frequencies inside the duct, greater efficiency is still needed to increase the number of internal elements.

A new numerical partition method partitioned matrix approach is now presented which allows far field acoustic problems to be subdivided into smaller independent and thus more manageable problems. This procedure can be incorporated in previously developed programs with minimal effort. Sample calculations for a two-dimensional rectangular coordinate soft wall duct with uniform flow are presented later to illustrate the method. Before discussing the partition approach, the boundary conditions used in a typical numerical acoustic analysis will be briefly reviewed.

Finite element or finite difference analyses usually require an acoustic pressure or velocity distribution as the entrance boundary condition and some assumed impedance as the exit boundary condition. For plane wave propagation without mean flow in a finite straight duct, the acoustic impedance at the outlet of the duct is nearly $\rho_0 c_0$ for dimensionless frequencies η greater than 1.5, as shown in Ref. 16. Figure 6(a) depicts the geometry

and appropriate boundary conditions for a rectangular duct with these conditions. For spinning or higher order modes, the exit impedance values of Refs. 1 or 3 could be used.

The basic idea for the partitioning approach comes from the marching technique developed in Ref. 17. As shown in Ref. 17, in regions where reflections are small, the $\rho_0 c_0$ exit impedance was nearly constant along the entire length of the duct. Thus, the internal portion of the duct and the far field can be separated into regions and solved independently. The exit pressure calculated in the first region is used as the initial condition for the pressure in the second region, and so forth.

For high frequency sound where reflections are small, the partition could be taken at the exit, as shown in Fig. 6(a). For low frequency sound or for an arbitrary input with multiple nodes, the partition should be moved from the exit to the far field where the $\rho_0 c_0$ impedance is valid, as shown in Fig. 6(b).

The number of partitions used in the far field could be as many as desired, as illustrated in Fig. 7. The total computer storage is reduced by approximately the square of the number of partitions. If seven partitions were used, this would be a storage reduction of about 50. Furthermore, since the solution times are roughly proportional to the total number of nodes cubed (Ref. 18, pg. 261), the total running time should also be reduced by a factor of 50.

To illustrate the capabilities of the partitioning technique, the noise attenuation at the optimum impedance (point of maximum attenuation in the impedance plane) is calculated using finite difference theory for a two dimensional rectangular duct with an L/H of 3.43, a uniform Mach number of 0.3 and a plane wave input.

Dimensionless frequencies of η equal to 1.5 and 2 are considered. As shown in Ref. 16, a dimensionless frequency of 1.5 is just sufficiently high so that a $\rho_0 c_0$ exit impedance is valid. In these two cases, as discussed in Ref. 17, the $\rho_0 c_0$ exit impedance is nearly constant along the entire duct. Therefore, the duct can be partitioned. Figure 8 shows the duct with seven assumed partitions represented by the dash vertical lines.

Figure 9 displays the calculated maximum sound power attenuations for η equal to 1.5 and 2. The number of axial grid points K have been varied to check for convergence. The results converge to the analytically predicted attenuation¹⁹ which apply to ducts of infinite length. Without partitions, approximately 100 axial grid points are required while with partitioning only 20 axial grid points are needed in each partitioned element. As mentioned in the body of the report, this reduces the storage requirement by a factor of 50 and the total running time also by a factor of 50. Of course, the method must be tested over a greater range of acoustic variables to check its validity.

Concluding Remarks

The finite element velocity potential program developed for NASA Lewis by Georgia Institute of Technology is suitable for handling low frequency acoustic wave propagation in ducts with area variations, centerbodies, and axial variations in wall impedance whenever irrotational flow gradients exist in a duct. Consequently, the program is ideally suited for handling low frequency acoustic wave propagation in a turbofan inlet in which the mean flow field is predominantly irrotational and two dimensional.

Unfortunately, as shown herein, the velocity potential program can not be used directly to estimate the effects of wall shear layers on acoustic propagation. However, a boundary layer correction based on the Goldstein-Rice analysis is suggested for predicting attenuation in soft wall ducts.

In some sample calculations for a variable area inlet, the combined effect of inlet curvature, and flow gradients was shown to have significant effects on the attenuation of a given acoustic liner for very low frequencies. The short center body did not seem to have such effect.

Finally, approaches are discussed that are actively being considered for extending the finite element solution to include the far field as well as the internal portion of the duct. A new matrix partitioning approach is presented that can be incorporated in previously developed programs which may allow the finite element calculation to be marched into the far field. The partitioning approach provides a large reduction in computer storage and running times.

References

1. Sigman, R. K., Majjigi, R. K., and Zinn, B. T., "Use of Finite Element Techniques in the Determination of the Acoustic Properties of Turbofan Inlets," AIAA Paper 77-18, Jan. 1977.
2. Abrahamson, A. L., "A Finite Element Algorithm for Sound Propagation in Axisymmetric Ducts Containing Compressible Mean Flow," AIAA Paper 77-1301, Oct. 1977.
3. Tag, I. A. and Lumsdaine, E., "An Efficient Finite Element Technique for Sound Propagation in Axisymmetric Hard Wall Ducts Carrying High Subsonic Mach Number Flows," AIAA Paper 78-1154, July 1978.
4. Baumeister, K. J. and Bittner, E. C., "Numerical Simulation of Noise Propagation in Jet Engine Ducts," NASA TN D-7339, 1973.
5. Quinn, D. W., "A Finite Difference Method for Computing Sound Propagation in Non-Uniform Ducts," AIAA Paper 75-130, Jan. 1975.
6. Baumeister, K. J., "Finite-Difference Theory for Sound Propagation in a Lined Duct with Uniform Flow Using the Wave Envelope Concept," NASA TP-1001, Aug. 1977.

7. Miller, B. A., Dastoli, B. J., and Mesoky, H. I., "Effect of Entry-Lip Design on Aerodynamics and Acoustics of High-Throat-Mach-Number Inlets for the Quiet, Clean, Short-Haul Experimental Engine," NASA TM X-3222, 1975.
8. Kagawa, Y., Yamabuchi, T. and Mori, A., "Finite Element Simulation of an Axisymmetric Acoustic Transmission System with a Sound Absorbing Wall," *Journal of Sound and Vibration*, Vol. 53, No. 3, Aug. 1977, 357-374.
9. Mungur, P. and Gladwell, G. M. L., "Acoustic Wave Propagation in a Sheared Fluid Contained in a Duct," *Journal of Sound and Vibration*, Vol. 9, No. 1, Jan. 1969, pp. 28-48.
10. Pai, Shih-I, Introduction to the Theory of Compressible Flow, D. Van Nostrand, Princeton, 1959.
11. Pridmore-Brown, D. C., "Sound Propagation in a Fluid Flowing Through an Attenuating Duct," *Journal of Fluid Mechanics*, Vol. 4, Pt. 4, Aug. 1958, pp. 393-406.
12. Goldstein, M. E., Aeroacoustics, McGraw-Hill, New York, 1976.
13. Savkar, S. D., "Propagation of Sound in Ducts with Shear Flow," *Journal of Sound and Vibration*, Vol. 19, No. 3, Dec. 1971, pp. 355-372.
14. Goldstein, M. and Rice, E., "Effect of Shear on Duct Wall Impedance," *Journal of Sound and Vibration*, Vol. 30, No. 1, Sep. 1973, pp. 79-84.
15. Meyer, W. L., Bell, W. A., Zinn, B. T., and Stalybrass, M. P., "Boundary Integral Solutions of Three Dimensional Acoustic Radiation Problems," *Journal of Sound and Vibration*, Vol. 59, No. 2, July 1978, pp. 245-262.
16. Majjigi, R. K.: Application of Finite Element Techniques in Predicting the Acoustic Properties of Turbofan Inlets, Ph. D. Thesis, Georgia Institute of Technology, submitted for approval 1979.
17. Baumeister, K. J., "Numerical Spatial Marching Techniques for Estimating Duct Attenuation and Source Pressure Profiles," 95th Meeting Acoustical Society of America, Providence, Rhode Island, May 1978, also published as NASA TM-78857, 1978.
18. McCracken, D. D. and Dorn, W. S., Numerical Methods and Fortran Programming, With Applications in Engineering and Science, Wiley, New York, 1964.
19. Motsinger, R. E., Kraft, R. E., Zwick, J. W., Vukelich, S. I., Minner, G. L., and Baumeister, K. J., "Optimization of Suppression for Two-Element Treatment Liners for Turbomachinery Exhaust Ducts," General Electric Company, Cincinnati, Ohio, R76AEG256, Apr. 1976. (NASA-CR-134997).

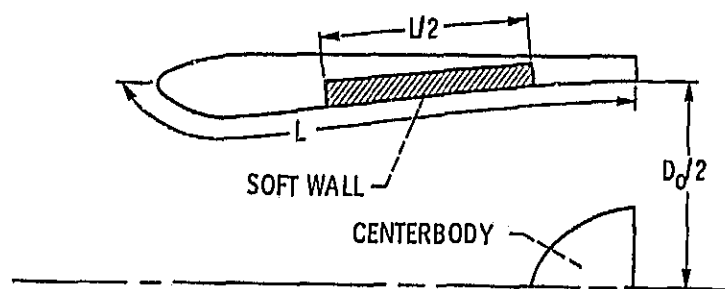


Figure 1. - Variable area Inlet.

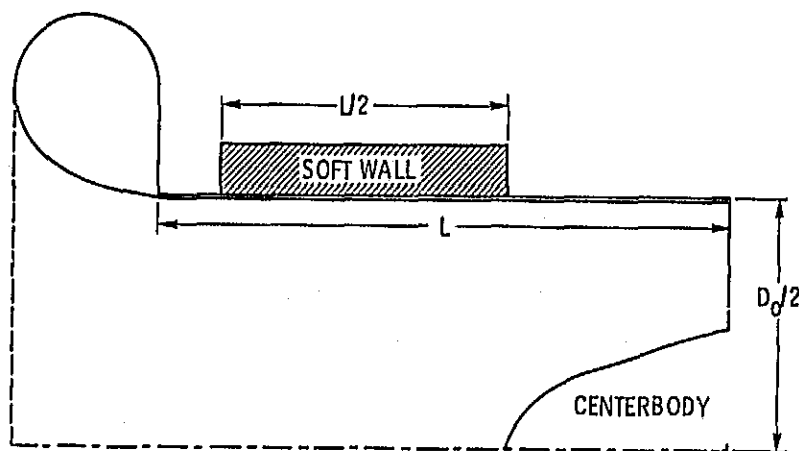


Figure 2. - Bellmouth Inlet.

ORIGINAL PAGE IS
OF POOR QUALITY

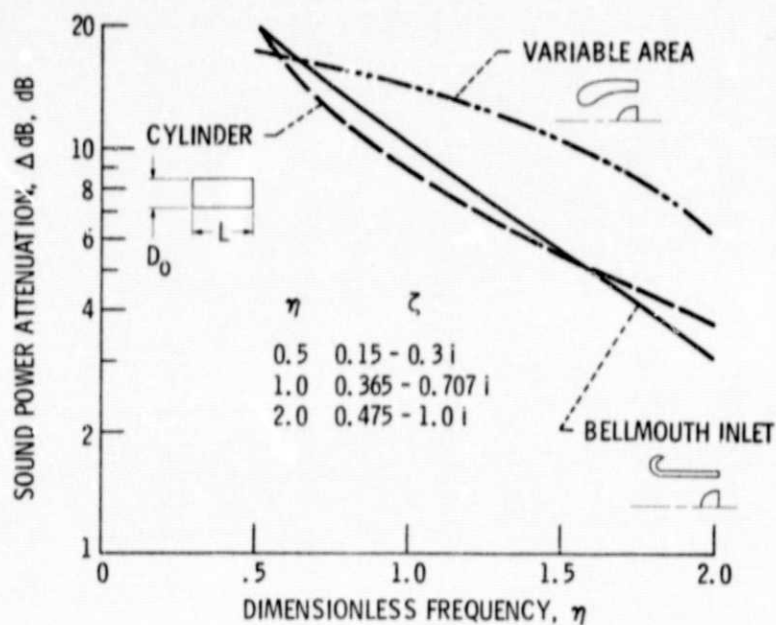


Figure 3. - Sound attenuation for inlets with a treatment U/D_0 of 0.5 for a plane acoustic velocity source with zero mean flow.

ORIGINAL PAGE IS
OF POOR QUALITY

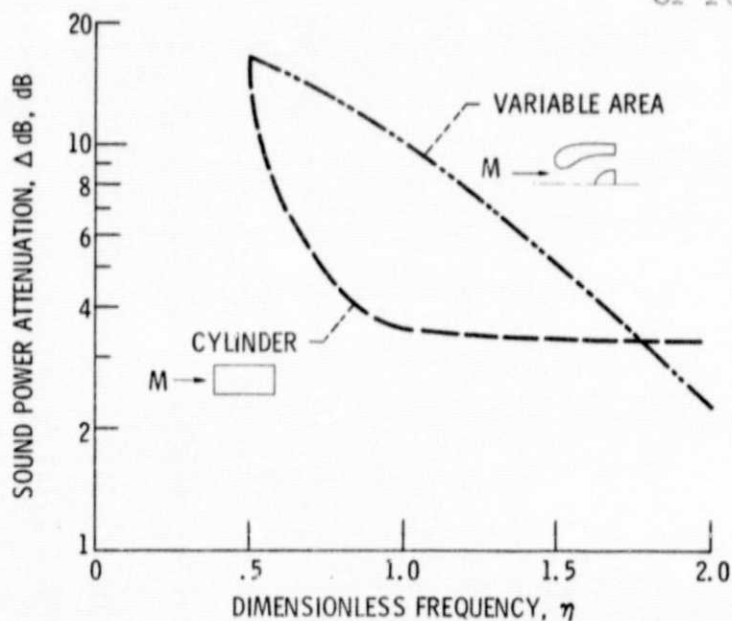


Figure 4. - Sound attenuation for inlets with a treatment U/D_0 of 0.5 for a plane acoustic pressure source with a fan face Mach number of 0.52.

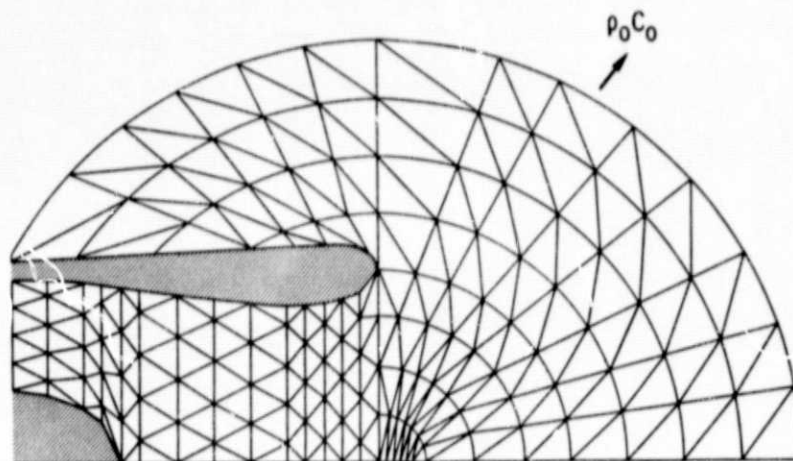
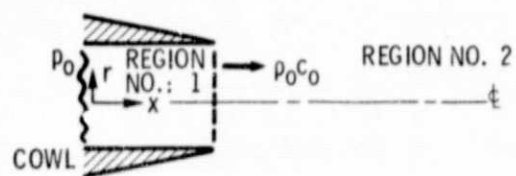
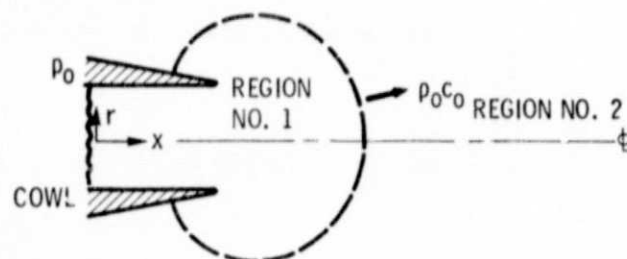


Figure 5. - Extending finite elements into far field.



(a) HIGH FREQUENCY APPROXIMATION.



(b) LOW FREQUENCY APPROXIMATION.

Figure 6. - Application of partitioning to engine inlets.

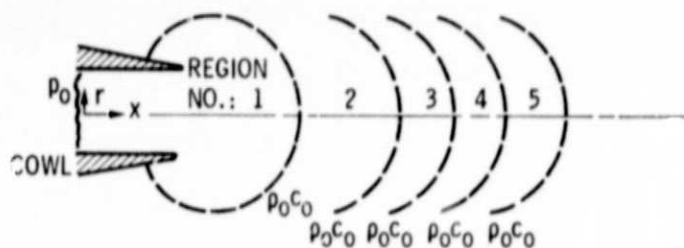


Figure 7. - Multi-partitions used in far-field analysis.

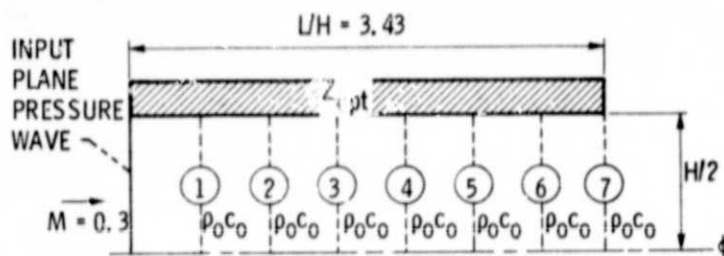


Figure 8. - Two-dimensional duct partitions.

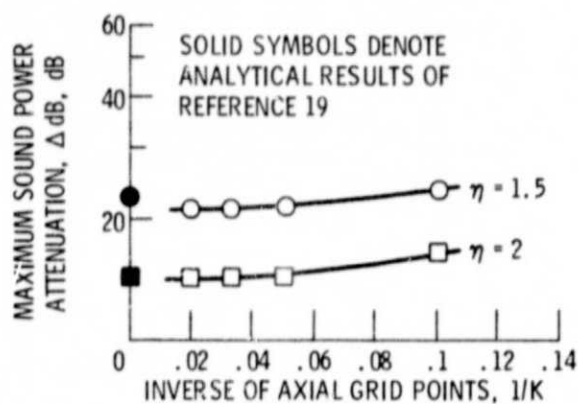


Figure 9. - Effect of number of axial grid point K on attenuation for seven partitions in a soft wall duct $L/H = 3.43$, $M = 0.3$ and wall impedance at optimum value for plane wave input.